HEFAT2010
7th International Conference on Heat Transfer, Fluid Mechanics and Thermodynamics
19-21 July 2010
Antalya, Turkey

NUMERICAL MODELING OF MULTIPHASE FLOW THROUGH MICRO- AND MACRO- PORES OF CLAY LANDFILL CAPS USING LATTICE BOLTZMANN METHOD

Kutay, M. E.* and Khire, M.
*Author for correspondence
Department of Civil and Environmental Engineering,
Michigan State University,
East Lansing, MI,
U.S.A,
E-mail: kutay@msu.edu

ABSTRACT

This paper presents a rigorous numerical model that simulates the saturated and unsaturated flow through fine-grained soils (clays) that contain micro-pores and macro-pores. Micro-pores are the pores where liquid can move vertically downwards as well as upwards due to capillary action and due to evaporative gradients. Macro-pores are large inter-clod voids, desiccation cracks, root penetrations, and other large size voids where water can only move downward due to gravity. Groundwater recharge from vadoze zone and solute or contaminant transport within vadoze zone and into the saturated aquifer is controlled by macro as well as micro pores. The model presented in this paper incorporates Brinkman's formulations into Lattice Boltzmann multiphase fluid flow model to simulate saturated and unsaturated flow through micro- and macro pores of clay landfill caps.

INTRODUCTION

Earthen covers are routinely used for capping municipal solid waste landfills (MSW) as well as to cap hazardous waste sites. There are about 1,500 MSW landfills that are currently active in the U.S. and several thousand old dumps and contaminated sites would need some form of capping in the near future. In order to control long term emissions and potential impacts from landfills, accurate prediction of liquid flow into waste as well gas emissions from landfills is critical. Often practitioners and researchers try to model the preferential flow in earthen caps by artificially increasing the hydraulic conductivity of the cap soils, this does not capture the physics of the flow through capillary pores and macro-pores accurately and often results in under-estimation of percolation and over-estimation of evapotranspiration (ET) or vice versa. Dual permeability models such as HYDRUS-2D (beta version), is an attempt to simulate the flow through the macro-pores using a soil-water and unsaturated hydraulic conductivity function that is not the same as that for the capillary pores or the soil matrix. However, the dual permeability model is numerically unstable and the authors believe that the flow through macro-pores cannot be accurately simulated by treating the macro-pores as capillary pores [1]. The flow in these pores is more like a flow in conduits with irregular shapes and hence Navier-Stokes equations are more appropriate and numerically more stable when solved using the Lattice Boltzmann method. This paper presents a rigorous numerical model based on the Lattice Boltzmann (LB) method to simulate the saturated and unsaturated flow through fine-grained soils (clays) that not only contain micro-pores but also macro-pores. The LB algorithms were developed to perform two-phase flow simulations to understand the movement of the water droplets within the macro-cracks as well as the suction of these droplets into the micro-cracks of the clay medium.

LATTICE BOLTZMANN METHOD FOR MODELING MULTIPHASE FLOW

The Lattice Boltzmann (LB) method has emerged as a versatile alternative to traditional finite-element and finite-difference Navier-Stokes solvers. The LB method has several advantages such as ease of implementation of boundary conditions and computational efficiency through parallel computing. The method naturally accommodates some of the boundary conditions such as a pressure drop across the interface between two fluids and wetting effects at the fluid-solid interface [2]. It was proven to be relatively accurate in simulating isothermal, incompressible flow at low Reynolds numbers [3].

The LB method approximates the continuous Boltzmann equation by discretizing physical space with lattice nodes and velocity space by a set of microscopic velocity vectors [4], [5]. The time- and space-averaged microscopic movement of fluid particles are modelled using molecular populations called distribution function. The distribution function defines the density and velocity of fluid molecules at each lattice node at each time step. Fluid particles travel on the lattice nodes based on the magnitude and direction of the distribution function components. Specific particle interaction rules are set so that the Navier-Stokes equations are satisfied. An illustration of generation of lattice for a given geometry and set of microscopic velocity vectors for the D3Q19 (3 dimensional, 19

microscopic velocity) and D2Q9 (2 dimensional, 9 microscopic velocity) LB models is shown in Fig. 1. Fig. 1a shows a 3D X-ray Computed Tomography image of a crack map. In Fig. 1b, the binary (black and white) image of pore space is shown for a 2D image slice for simplicity. In our implementation of LB method, the lattice nodes are generated at the center of each white pixel (or voxel in 3D) and microscopic velocity vectors are defined as shown in Fig. 1c (for 3D LB model) and Fig. 1d (for 2D LB model).

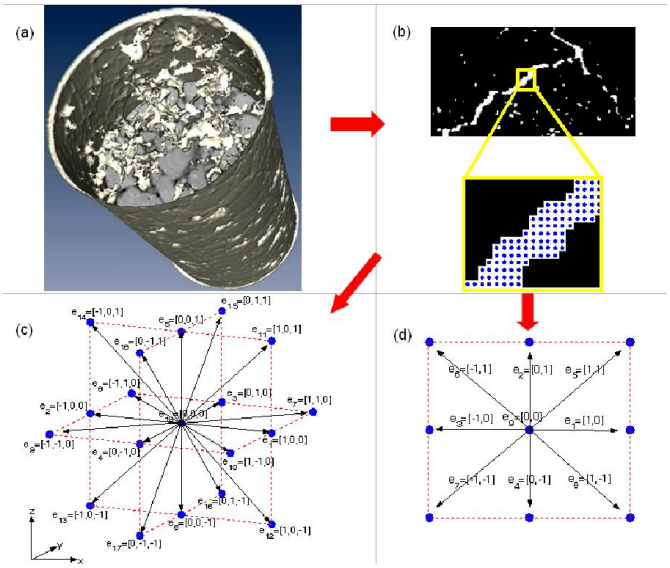

Figure 1 (a) X-ray CT image of soil grains (b) binary image (black areas represent the solid, and white areas represent the air space) and generation of lattice nodes at the center of each white pixel, (c) D3Q19 and (d) D2Q9 lattice microscopic velocity directions defined at each node.

Extensive description of our implementation of single-phase 3D LB models can be found elsewhere ([6], [7]), therefore it will not be repeated here. Scope of the research presented in this paper includes only the simulation of unsaturated water flow within the macro and micro-pores of soil medium. To accomplish this, a multiphase LB model has been implemented to simulate the collective behaviour of water and air within the macro-pores of soil.

LATTICE BOLTZMANN EQUATIONS FOR MULTIPHASE FLOWS

Numerical simulation of multiphase (or multi-component) fluid flow is challenging because of difficulties in modeling interface dynamics as well as the wetting effects of each fluid on solids. One of the primary advantages of the LB method is that it can naturally incorporate interactions between the different fluids and between fluids and solids through specific interaction rules adopted using the concept of distribution function [8]. The distribution function ($\mathrm{F}_\mathrm{i}^\sigma$) represents the molecular populations and defines the time- and space-averaged microscopic movement of fluid molecules (herein called particles). The time dependent movement of fluid particles at each lattice node satisfies the following particle propagation equation [9]:

$$\mathrm{F}_\mathrm{i}^\sigma(\mathbf{x}+\mathbf{e}_i, t+1) = \mathrm{F}_\mathrm{i}^\sigma(\mathbf{x},t) - \frac{1}{\tau_\sigma}\left[\mathrm{F}_\mathrm{i}^\sigma(\mathbf{x},t) - \mathrm{F}_{i(eq)}^\sigma(\mathbf{x},t)\right] - g_i^\sigma \quad (1)$$

where $\mathrm{F}_\mathrm{i}^\sigma$ is the distribution function of the fluid component σ, $\mathrm{F}_{i(eq)}^\sigma$ is the equilibrium distribution function of the fluid component σ, and $\mathbf{e}_\mathrm{i}$ is the microscopic velocity at lattice node $\mathbf{x}$ at time t, respectively, and τ is the relaxation time which is a function of each fluid's kinematic viscosity (i.e., $\nu^\sigma = c_s^2(\tau_\sigma - 0.5)$ where $c_s = 1/\sqrt{3}$ is the lattice speed of sound for D2Q9 and D3Q19 models). The subscript i represent the lattice directions around the node as shown in Fig. s 1c and 1d. The g_i^σ in Eq. 1 is the body force term and has the following form [2]:

$$g_i^\sigma = -\frac{w_i}{c_s^2}\rho_m^\sigma(\mathbf{e}_i \cdot \mathbf{g}) \quad (2)$$

where $\mathbf{g}$ is the acceleration field due to a body force and w_i is the weight factor in the i^{th} direction and ρ_m^σ is the (number) density of the lattice node (Eq.4). Weight factors vary for different LB models [7]. The weight factors (w_i) for the D2Q9 LB model are: w_9 =16/36 for rest particle, w_i=4/36 ($1 \le i \le 4$) for particles streaming to the face-connected neighbors and w_i=1/36 ($5 \le i \le 8$) for particles streaming to the edge-connected neighbors. The weight factors are derived based on the lattice type (DxQy) and the derivations can be found in [10].

Equilibrium distribution functions ($\mathrm{F}_{i(eq)}^\sigma$) for different models were derived by [11]. The function is given in the following form for D3Q19 and D2Q9 models:

$$\mathrm{F}_{i(eq)}^\sigma = w_i\,\rho_m^\sigma\left[1 + 3(\mathbf{e}_i \cdot \mathbf{u}^\sigma) + \frac{9}{2}(\mathbf{e}_i \cdot \mathbf{u}^\sigma)^2 - \frac{3}{2}(\mathbf{u}^\sigma \cdot \mathbf{u}^\sigma)\right] \quad (3)$$

where $\mathbf{u}^\sigma$ is velocity of the σ^{th} fluid component and ρ_m^σ is the (number) density of the lattice node which is the scalar summation of each component of the distribution function as follows:

$$\rho_m^\sigma = \sum_i \mathrm{F}_\mathrm{i}^\sigma \quad (4)$$

Interaction between Different Fluids

In order to model the surface tension between different fluids, we adopted one of the most common methods, called Shan-Chen (SC) model [9]. In this model, first, the following rate of change of momentum is computed at each node:

$$\frac{d\mathbf{U}^\sigma}{dt}(\mathbf{x}) = -\psi^\sigma(\mathbf{x})\sum_{\sigma'}^{S} G_{\sigma\sigma'}\sum_i \psi^{\sigma'}(\mathbf{x}+\mathbf{e}_i)\mathbf{e}_i \quad (5)$$

where $\mathbf{U}^\sigma$ is the momentum of liquid σ, $G_{\sigma\sigma'}$ is a parameter used to define the interaction strength between liquid phases σ and σ' and $\psi^\sigma(\mathbf{x})$ is a function of the density for the σ^{th} phase at the node **x.** Similar to Shan-Chen's implementation, we chose $\psi^\sigma(\mathbf{x}) = \rho_0[1 - \exp(\rho/\rho_0)]$ where ρ_0 is a constant. After calculating the rate of change of momentum using Eq. 5, the net momentum of each fluid component is shifted to separate different fluids as follows:

$$\rho^\sigma(\mathbf{x})\mathbf{u}^\sigma(\mathbf{x}) = \rho^\sigma(\mathbf{x})\mathbf{u}(\mathbf{x}) + \tau_\sigma\frac{d\mathbf{U}^\sigma}{dt}(\mathbf{x}) \quad (6)$$

where ρ^σ is the density and $\mathbf{u}$ is the average velocity of different fluids at each node and they are calculated using the following relations:

$$\rho^{\sigma} = m^{\sigma}\rho_m^{\sigma} \tag{7}$$

$$\mathbf{u} = \frac{\sum_{\sigma=1}^{S} m^{\sigma}\sum_i \mathrm{F}_i^{\sigma}\mathbf{e}_i/\tau_{\sigma}}{\sum_{\sigma=1}^{S}\rho^{\sigma}/\tau_{\sigma}} \tag{8}$$

where m^{σ} is the molecular mass of the σ^{th} fluid component and S is the number of fluids. Then the computed $\mathbf{u}^{\sigma}(\mathbf{x})$ in Eq. 6 is utilized in the $\mathrm{F}_{i(eq)}^{\sigma}$ equation in Eq. 5.

Steps of the LB Algorithm

A detailed description of the steps of single phase LB algorithm is presented in Kutay et al. [7]. The steps for multiphase fluids are very similar to those of a single phase. A brief description of the steps is as follows:

1. Assign density and velocity to all lattice nodes and calculate initial equilibrium distribution, $\mathrm{F}_{i(eq)}^{\sigma}(\mathbf{x}, t=0)$ using Eq. 3. Then assume initially $\mathrm{F}_i^{\sigma}(\mathbf{x}, t=0) = \mathrm{F}_{i(eq)}^{\sigma}(\mathbf{x}, t=0)$.
2. Propagate the fluid particles to neighboring nodes by calculating new (non-equilibrium) distribution functions of all nodes using Eq. 1.
3. Impose boundary conditions at the solid-fluid interface and at domain boundaries.
4. Calculate new densities and velocities of the nodes using Eq.'s 7 and 8.
5. Calculate the rate of change of momentum using Eq. 5 and modify the velocities using Eq. 6.
6. Calculate new equilibrium distribution function of each node using Eq. 3.

Repeat steps 2 through 6 until the mass balance tolerance is met.

Boundary Conditions at the Domain Boundaries

In the propagation step of the LB algorithm, all components of the non-equilibrium distribution function are computed at each node except at nodes that are located at the boundaries of the domain (i.e., for D2Q9 model: north, south, east and west nodes). These components can be calculated by setting either pressure or velocity boundary condition, which are described in Kutay et al. [7]. Also, periodic boundary conditions can also be utilized where distribution function components exiting from one side of the domain enters from the opposite side. Another useful method is utilizing Grad's approximation method [5]. This method allows the fluid to *flow out* of the domain. In this method, each missing component of the distribution function is computed using the following formula:

$$\mathrm{F}_i^{*} = w_i\left[\rho + \frac{\rho u_{\alpha} e_{i\alpha}}{c_s^2} + \frac{1}{2c_s^4}(\mathrm{P}_{\alpha\beta} - \rho c_s^2\delta_{\alpha\beta})(e_{i\alpha}e_{i\beta} - c_s^2\delta_{\alpha\beta})\right] \tag{9}$$

where ρ is the density of the node, and w_i is the weight factor in the i^{th} direction, u is the (macroscopic) velocity of the node, e_i is the microscopic velocity, c_s is the lattice speed of sound and δ is the kronecker delta, repeating subscripts α and β represent the summation in tensor notation (each representing a component of the vector) and $\mathbf{P}_{\alpha\beta}$ is as follows:

$$\mathrm{P}_{\alpha\beta} = \sum_{i=1}^{9}\mathrm{F}_i e_{i\alpha}e_{i\beta} \tag{10}$$

INCORPORATION OF HYDRAULIC CONDUCTIVITY AT PERMEABLE SOLID REGIONS (MICRO-CRACKS) IN LB MODEL

In the clay cap test sections to be modeled in this study, the flow in macro-pores (or "cracks") as well as the flow in the micro-pores of the clay will be modeled. When the clay is not fully saturated, there is suction in micro-pores of the clay which draws the water flowing in the cracks. This suction force (i.e., suction head) will decrease over time as the moisture content within the micro-pores increase. In addition, large surface area of micro-pores of the clay medium acts as a resistive force limiting the water seepage into the micro-pores. Furthermore, this resistive force will decrease (i.e., the hydraulic conductivity will increase) with increasing moisture content.

Application of Brinkman's Equation

The Brinkman equation [12] is a generalization of Darcy's law that allows matching of the boundary conditions at an interface between the larger pores and the permeable medium and has the following form [2]:

$$\nabla\mathbf{P} = \mu\nabla^2\mathbf{v} - \frac{\mu}{K}\mathbf{v} \tag{12}$$

where μ is the fluid dynamic viscosity (Pa-s), K is the intrinsic permeability (mm^2) and the $\mathbf{v}$ is the velocity (mm/s). Given that the kinematic viscosity $\nu=\mu/\rho$ and the hydraulic conductivity, k (mm/s) is $k = K\gamma/\mu$ (γ= unit weight of fluid), the Eq. 12 can be rewritten as follows:

$$\nabla\mathbf{P} = \mu\nabla^2\mathbf{v} - \frac{\gamma}{k}\mathbf{v} \tag{13}$$

It should be noted that the first part of Eq. 13 is actually the Stokes' equation, which is solved by the LB formulations, whereas the second part is the Darcy's equation. In macro-pore space, since k is infinity, second part of Eq. 13 goes to zero and the Stokes' equation holds. Whereas when the fluid is traveling within the micro-pores of a permeable medium, the second component is dominant.

The Eq. 13 was implemented in LB formulations using the method suggested by Martys [13], where a body force term applied to the permeable solid regions that causes momentum sink. To accomplish this, body force acceleration ($\mathbf{a}_k$) due to the hydraulic conductivity is defined as follows:

$$\mathbf{a}_k = -\frac{\mu}{\rho K}\mathbf{v} = -\frac{\gamma}{\rho k}\mathbf{v} = -\frac{g}{k}\mathbf{v} \tag{14}$$

where ρ is the density of fluid and g is the gravitational acceleration (g=9.81 m/s^2). This body force acceleration is added to the body force term in Eq. 2 as follows:

$$\mathbf{g} \Leftarrow \mathbf{g} + \mathbf{a}_k \tag{15}$$

In addition to application of Eq. 15 that causes momentum sink in the permeable regions, the relaxation time (τ_{σ}) must also be modified to match the shear stress at the free fluid/ permeable medium interface. This is accomplished by defining an effective viscosity parameter, μ_e, for the permeable medium and using the following relaxation parameter in this zone:

$$\tau_{\sigma(e)} = 3\frac{\mu_e}{\rho} + 0.5 \tag{16}$$

where $\tau_{\sigma(e)}$ is the (modified) relaxation time used in the lattice nodes in the permeable regions.

Validation of the LB model

An analytical solution for Equation 12 for simple shearing flow above a porous flat plane (Fig.2) is given in [14] as follows:

$$u_x(y) = a + by \qquad (0 < y < d_1)$$
$$u_x(y) = a\exp\left(\frac{y}{\sqrt{\mu_e K/\mu}}\right) \qquad (-d_2 < y < 0) \tag{17}$$

where u_x is the horizontal velocity, d_1 and d_2 are the distance above and below the surface of porous media (Fig.2), K is the intrinsic permeability (mm^2), μ_e is the effective viscosity parameter, and the coefficients a and b are given as follows:

$$a = \frac{V_x}{1+\sqrt{(\mu_e/\mu)}(d_1/\sqrt{K})}, \qquad b = \sqrt{\frac{\mu_e}{\mu}}\frac{a}{\sqrt{K}} \tag{18}$$

LB simulations were performed to model the shearing flow shown in Fig. 5. A horizontal velocity of 600 mm/s was assigned at the north surface of the domain. Zero velocity boundary condition was assigned at the south and periodic boundary conditions were set in the x-direction (i.e., for east and west sides of the domain). Simulations were performed at three permeability levels: k = 0.1, 1 and 5 mm/s for the porous media. As shown in Figure 2, an excellent agreement was observed between the LB simulations and analytical solution of Brinkman equation.

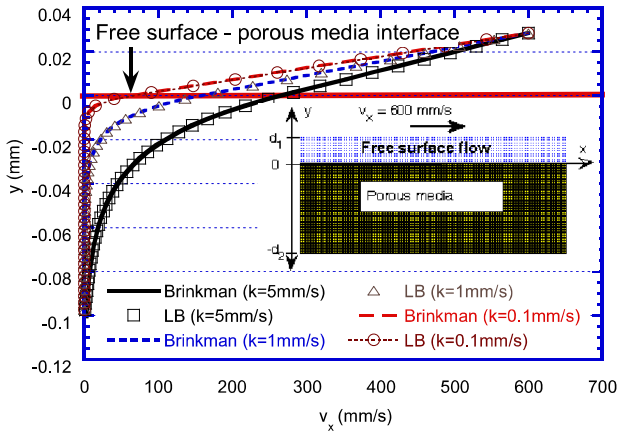

Figure 2. Comparison between the analytical solution of Brinkman equation and the LB simulations.

TWO-PHASE FLUID FLOW SIMULATIONS THROUGH MACRO PORES OF A CLAY LANDFILL CAP

In order to test the multiphase LB algorithms, preliminary two-phase simulations were conducted on approximate crack geometry of a specimen obtained from the field (Fig. 3a). The specimen was subjected to a rhodamine tracer test to determine the relative location of the interconnected macro-pore structure. The specimen was cut into half for imaging (Fig. 3b). From the image, location(s) of the crack(s) was determined and the binary image was obtained (Fig. 3c).

The LB simulations of water flow through an initially dry (i.e., filled with air) crack structure were performed. A constant influx of water at the surface was assumed and the downward movement of the water was simulated by applying a body force acceleration of 9.81 m/s^2. The interaction strength ($G_{\sigma\sigma'}$ in Eq. 5) between the water and air was assumed to be 2.1. This number was selected via numerous trials until the best phase separation (without diffusion) between the water and air. Reducing this parameter causes two fluids to diffuse into each other and mix.

Fig. 3d shows the three snapshots of the simulation results where the evolution of the water migration within the crack can be seen. Entire simulation can be viewed at Kutay URL1 [15]. Fig. 3d also shows the simulated precipitation and percolation where the delay in percolation as well as the difference in the slope of the cumulative percolation compared to the cumulative precipitation is noticeable. It is noted that while the simulation was performed for two-phase flow, this graph only illustrates the percolation of water. Similar graphs can also be developed for the air phase. The vertical scale of the images shown in Fig. 3d is about 100 mm. The slope of percolation plot is the liquid flux which will depend upon the size and distribution of macro-pores and its connectivity with micro-pores. It will also depend upon the rate of precipitation, and evaporative gradients. These processes will be modeled in a future study to capture the hydrology of clay caps containing macro-pores.

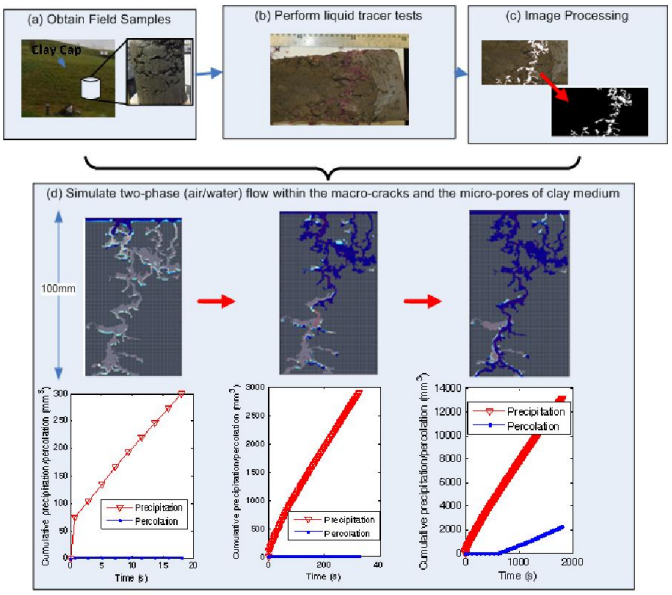

Figure 3. Illustration of two-phase flow simulation results for clay sample collected from the test sections from the instrumented clay cap located in Detroit-MI.

CONCLUSION

Landfill caps made of compacted clay often have large interconnected macro-pores due to desiccation or over-compaction. This causes large quantities of water to seep into the waste material, which in turn lead to development leachate. Therefore, estimation of quantity of percolation from the clay caps is very important. This paper presented implementation of a multiphase fluid flow simulation technique, the Lattice Boltzmann (LB) method, to simulate the unsaturated water flow within the macro- and micro-pores of landfill clay caps. The LB method was implemented along with the addition of

Brinkman's formulation to be able simulate the flow within the micro-pores of the clay medium. The LB model was validated against analytical solution of simple shearing flow above a porous space. An excellent agreement between the LB simulations and the analytical solution was observed. In addition, preliminary simulations of two-phase (unsaturated) water flow through the internal crack structure of a clay sample obtained from the field were presented.

REFERENCES

[1] Hardt, C. (2008). "Numerical Evaluation of Preferential Flow Through Evapotranspirative Landfill Covers." *Masters Thesis*, Dept. of Civil and Environmental Engineering, MSU, East Lansing, Mich., 67 p.

[2] Martys, N.S. and Hagedorn, J.G. (2002). "Multiscale Modeling of Fluid Transport in Heterogeneous Materials Using Discrete Boltzmann Methods." *Materials and Structures*. 35: 650-659.

[3] Succi S. (2001). *The Lattice Boltzmann Equation: for Fluid Dynamics and Beyond*. Series Numerical Mathematics and Scientific Computation, Oxford University Press, Oxford-New York.

[4] McNamara, G. and Zanetti, G. (1988). "Use of the Boltzmann Equation to Simulate Lattice-Gas Automata." *Phys. Rev. Lett*. 61: 2332-2335.

[5] Maier R.S., Bernard R.S., Grunau, D.W. (1996). "Boundary Conditions for the Lattice Boltzmann Method." Physics of Fluids. 8 (7): 1788–801.

[6] Kutay, M.E., Aydilek, A.H., Masad, E., and Harman, T. (2007a). "Computational and Experimental Evaluation of Hydraulic Conductivity Anisotropy in Hot Mix Asphalt." International Journal of Pavement Engineering. 8 (1): 29-43.

[7] Kutay, M.E., Aydilek, A.H. and Masad, E. (2006). "Laboratory Validation of Lattice Boltzmann Method for Modeling Pore-scale Flow in Granular Materials." Computers and Geotechnics. 33: 381-395.

[8] Martys, N.S. and Chen, H., (1996). "Simulation of Multicomponent Fluids in Complex Three-dimensional Geometries by the Lattice Boltzmann Method", Physical Review E. 53 (1): 743-750.

[9] Shan, X. and Chen, H., (1993). "Lattice Boltzmann Model for Simulating Flows with Multiple Phases and Components." Physical Review E. 47 (3): 1815-1820.

[10] Wolf-Gladrov, D. A. (2000). "Lattice-Gas Cellular Automata and Lattice Boltzmann Models: An Introduction." Springer, Berlin.

[11] He, X. and Luo, L. (1997). "Theory of Lattice Boltzmann Method: From the Boltzmann Equation to the Lattice Boltzmann." Phys. Rev. E. 56: 6811-6817.

[12] Brinkman, H.C. (1949). "A Calculation of Viscous Force Exerted by a Flowing Fluid on a Dense Swarm of Particles." Applied Scientific Research A. 1 (1): 27-34.

[13] Martys, N.S.(2001) "Improved Approximation of Brinkman Equation using a Lattice Boltzmann Method", *Physics of Fluids*, Vol. 13, No 6, pp 1807-1810.

[14] Martys, N.S., Benz, D.P., and Garboczi, E.J., (1994) "Computer simulation study of the effective viscosity in Brinkman's equation", *Physics of Fluids*, Vol. 6, No 4.

[15] Kutay, M.E. URL 1 (2009). http://www.egr.msu.edu/~kutay/LBsite/twophasefl.htm